Near Infrared Spectral Changes of Cytochrome aa_3 during Potentiometric Titrations

Richard W. Hendler,* Paul A. Harmon,‡ and Ira W. Levin‡

*Laboratory of Cell Biology, National Heart, Lung, and Blood Institute, and ‡Laboratory of Chemical Physics, National Institute of Diabetes and Digestive and Kidney Diseases, National Institutes of Health, Bethesda, Maryland 20892 USA

ABSTRACT Singular value decomposition (SVD) was used to deconvolute the spectral changes occurring in the near infrared region during potentiometric titrations of cytochrome aa_3. Overall oxidized minus reduced difference spectra revealed a broad absorbance feature centered near 830 nm with an apparent E_m near 250 mV. However, SVD did not isolate any spectral species with an absorbance centered near 830 nm. It was found that the spectral changes occurring in the wavelength region from 650 to 950 nm were associated mainly with cytochromes a and a_3. It was concluded that the absorbance at 830 nm should not be used as an independent measure of the concentration of Cu_A in cytochrome aa_3.

INTRODUCTION

In their monograph on cytochrome oxidase, Wikström et al. (1981) state that the optical absorbance at ~830 nm can be used as a probe for the redox state of the Cu_A center. The belief that Cu_A is a major contributor to this band in oxidized cytochrome aa_3 goes back about 30 years (Wharton and Tzagaloff, 1964). The experimental basis for the conclusion rests largely on the correlation between EPR changes and the optical absorbance at ~830 nm seen during potentiometric titrations (Tsudzuki and Wilson, 1971), upon photolysis of the mixed-valence CO compound in the presence of formate (Boelens and Wever, 1980), and under different conditions of oxidation and reduction (Beinert et al., 1980). Additional support is based on spectroscopic studies employing magnetic and natural circular dichroism (Eglinton et al., 1980; Greenwood et al., 1983). More recently, Dr. B. C. Hill reported at the 38th annual meeting of the Biophysical Society in New Orleans, 1994, that an oxidized minus reduced difference optical spectrum of the *Bacillus subtilis* oxidase aa_3-600, which lacks a binding site for Cu_A, shows an absence of the 830 nm feature. This is also consistent with the view that the principal contributor to the absorbance at 830 nm is Cu_A.

From the earliest observations, because of effects caused by CO, it was suspected that cytochrome a_3 contributes a small amount of absorbance to this region (Wharton, 1964; Tsudzuki and Wilson, 1971). Boelens and Weaver (1980), on the other hand, found no effect of CO and therefore discounted any contribution by cytochrome a_3. Eglinton et al. (1980) concluded that although cytochrome a_3 does contribute absorbance to the 830 nm region, the major part of the absorbance comes from Cu_A. More recently, Einarsdottir et al. (1992) and Rich et al. (1992) presented convincing new evidence that cytochrome a_3 provides a specific absorbance at ~785 nm. Einarsdottir et al. (1992) also describe an absorbance feature at ~710 nm that they attribute to cytochrome a. Hallen and Brzezinski (1994) reported that kinetic changes at 830 nm during the oxidation of one electron-reduced cytochrome aa_3 could be attributed mainly to heme absorption.

During the past two decades, potentiometric and kinetic characterizations of Cu_A have been based on the assumption that the absorbance at ~830 nm can be attributed mainly to Cu_A (e.g., Tiesjema et al., 1973; Thornstrom et al., 1988; Morgon et al., 1989; Hill, 1991, 1994; and references in Wikström et al., 1981). In the most recent publication (Hill, 1994), the reference of Greenwood et al. (1983) was cited as justification for the view that "Cu_A is the only chromophore with a major contribution at this wavelength" (i.e., 830 nm). However, in Greenwood et al. (1983), a caveat is given: "Although we have shown in the present work that Cu_A^{2+} totally dominates the low temperature m.c.d. spectra of the oxidized enzyme between 700 and 900 nm, this does not enable us to state that Cu_A^{2+} must therefore dominate the absorption spectrum in this region."

In the present study, we use the method of singular value decomposition (SVD) combined with spectral potentiometric titration data to determine the degree of confidence that one may place on attributing absorbance changes at ~830 nm to changes in the redox state of Cu_A. Our conclusion is that absorbance changes in the 830 nm region *cannot* be used as indicative of the change in redox state of Cu_A.

In view of our findings, it is worthwhile to recall comments made by Caughey nearly thirty years ago (1966) that have been mostly ignored. He stated that because heme components can be expected to contribute significantly to the 830 nm absorption in cytochrome oxidase and that changes in the copper components of the oxidase could affect the heme absorbance, it is questionable to associate the 830 nm absorbance with Cu alone. Ten years later, in a further review

Received for publication 5 May 1994 and in final form 19 July 1994.

Address reprint requests to Dr. Richard W. Hendler, Mem. Enzy./Lab. Cell Biol., NHLBI, National Institutes of Health, Bldg. 3, Rm. B1-06, Bethesda, MD 20892-0003. Tel.: 301-496-2610; Fax: 301-402-1519; E-mail: rwh@helix.nih.gov.

Dr. Harmon's current address: Merck Manufacturing Division, Merck and Co., West Point, PA 19486.

0006-3495/94/12/2493/08 $2.00

of the evidence linking the 830 nm absorbance with the redox state of Cu, he concluded that it was not shown that copper-(II) is a unique contributor or even a contributor at all to the 830 nm band intensity (Caughey, 1976).

EXPERIMENTAL PROCEDURES AND ANALYSIS

General

Bovine cytochrome aa_3 was prepared by the method of Yoshikawa et al. (1977). These preparations consisted of ~0.9 mM heme A in 0.01 M sodium phosphate buffer (pH 7.4) and were stored aerobically at −90°C in 22 μl aliquots. Specific details about the redox mediators used, method of solution potential control, optical spectrometer, and accumulation of data are contained in Harmon et al. (1994a, b). For the experiment shown in Fig. 1, the final concentrations in a total volume of 1.2 ml of 63 mM sodium phosphate and 125 mM KCl at pH 7.2 were: cytochrome oxidase, 17 μM; 1,2-naphthoquinone and diaminodurene at 100 μM each; and $K_3Fe(CN)_6$, quinhydrone, and diaminodurene at 200 μM each. For the experiment shown in Fig. 2, the concentrations of cytochrome oxidase and mediators were doubled *and* hydroxymethyl ferrocene was substituted for $K_3Fe(CN)_6$.

Singular value decomposition (SVD) analysis

The data to be analyzed consist of a series of overlapping spectra, each of which is changing with voltage as described by the Nernst equation, its midpoint potential, E_m, and "n" value. Each composite spectrum is represented by a column of numbers (i.e., absorbances) contained in 365 rows (i.e., wavelengths) for the experiment shown in Fig. 1, and 510 rows for the experiment shown in Fig. 2. A single experiment therefore produces a matrix with 365 or 510 rows and 25 columns, one for each voltage tested. The object of SVD is to deconvolute the matrix of raw experimental data into two factor matrixes, one that contains all of the individual difference spectra for each component and the other that contains the proper Nernst expressions to describe their redox behavior. The procedure for accomplishing this is based in linear algebra. A complete description of the theory of SVD with illustrations in its usage is described in Hendler and Shrager (1994), and it is recommended that readers who would like more background and understanding of the procedure consult this paper. Below, a very brief synopsis will be presented.

Let A be the matrix containing the raw data, D the matrix whose columns contain the starting, maximally reduced spectrum for the total mixture plus a difference spectrum for each component, and F the matrix whose columns contain the proper Nernst expressions for each component plus a column of "1s" to represent the reference (totally reduced) spectrum. Then,

$$A = DF^{T} \quad (1)$$

where the superscript T denotes the transpose of the matrix. SVD provides a means for deducing both D and F. The original matrix is factored by SVD into three matrices.

$$A = USV^{T} \quad (2)$$

The U and V matrices contain basis sets of orthonormal eigenvectors which

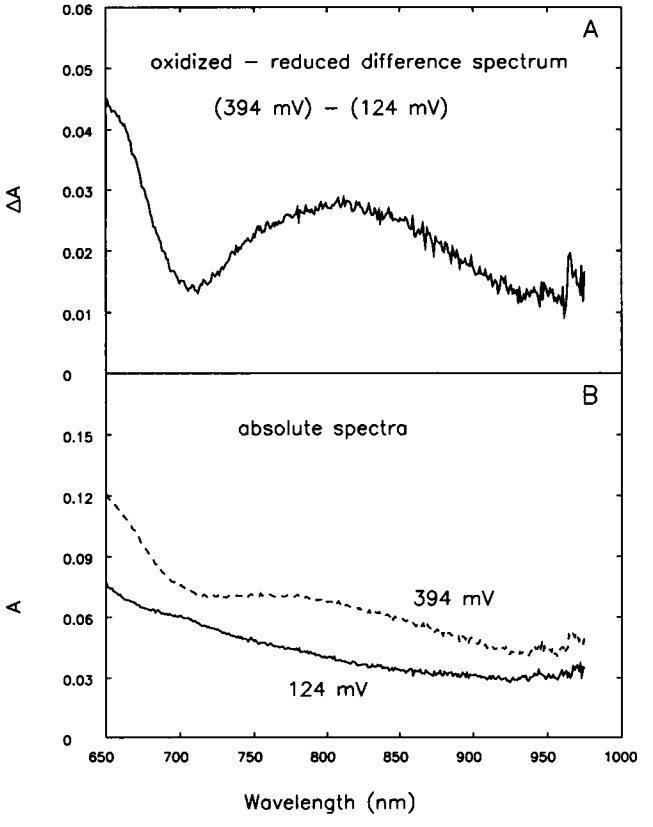

FIGURE 1 Near infrared spectra of cytochrome aa_3 at two solution potentials. A potentiometric titration was performed from 124 to 394 mV (vs. SHE) in 24 steps. Spectra were taken from 623 to 975 nm in 364 steps. The overall difference spectrum (394–124 mV) is shown in *A*, and the individual spectra at 394 and 124 mV are shown in *B*. See Experimental Procedures and Analysis for further details.

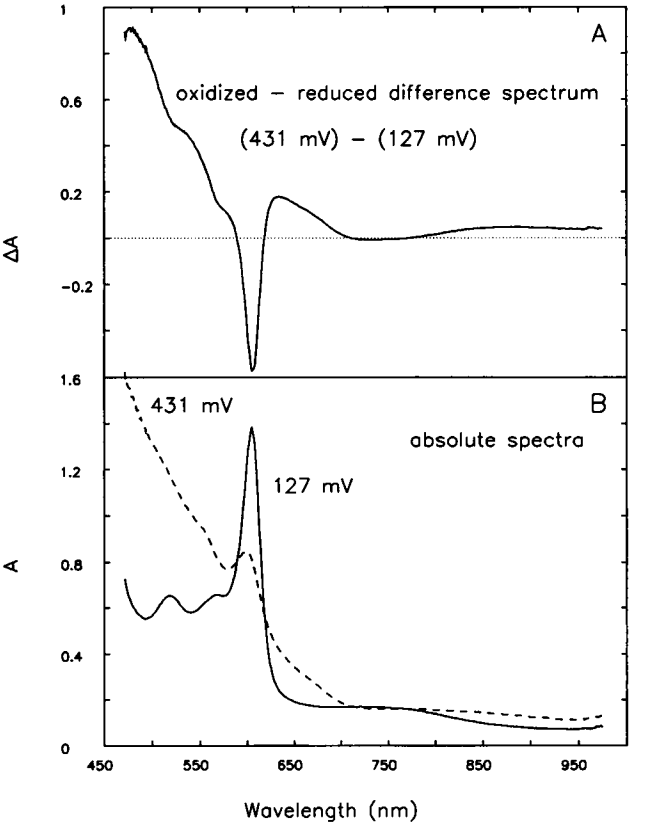

FIGURE 2 Visible and near infrared spectra of cytochrome aa_3 at two solution potentials. A potentiometric titration was performed from 127 to 431 mV (vs. SHE) in 24 steps. Spectra were taken from 471 to 975 nm in 509 steps. The overall difference spectrum (431–127 mV) is shown in *A*, and the individual spectra at 431 and 127 mV are shown in *B*. See Experimental Procedures and Analysis for further details.

separate the column (i.e., spectral) space and row (i.e., titration) space of the original matrix, respectively.

S is a diagonal matrix whose elements contain weight (singular) values for the columns of U and V. It is apparent that D and F are related to U, S, and V.

$$DF^T = USV^T. \quad (3)$$

$$D = USH, \quad (4)$$

where

$$H = V^T F^{T+}, \quad (5)$$

where the superscript + denotes the pseudo-inverse of F^T. In effect, H contains the coefficients that specify how to mix the weighted spectral columns in U to form the desired spectra in D. H is determined by curve-fitting the columns of V, using combinations of Nernstian expressions. The columns of V, when plotted against the actual voltages used in the titration, undergo changes in direction. In theory, each separate component should provide one change of direction. This is a strong aid that indicates the number of different components that are present. In arriving at a solution, several different fitting models should be tried. These should use the indicated number of components deduced from the observed changes in direction of the V column vectors as well as models with more and less components. The "n" values for each component may be varied as well.

In this particular application of SVD, many different models were tried to fit the data. These involved changes in the number of components from two to seven and the use of different n values in models with a fixed number of components. The criteria used for selection of the best fits were: 1) goodness of fit; 2) in cases where the α absorbance feature of cytochrome aa_3 was present, that the derived E_ms were consistent with previously established values for the heme centers (Hendler and Westerhoff, 1992; Harmon et al., 1994a); and 3) in cases where the α absorbance region was omitted, that the E_m values were consistent with the E_m values established on the basis of criteria 1) and 2) above, and that the derived difference spectra in the near infrared region were, in all cases, essentially the same.

RESULTS

Fig. 1 *A* shows a broad absorbance feature near 830 nm in an oxidized minus reduced spectrum covering the voltage range of 124–394 mV. This absorbance feature is commonly attributed to the spectrum for oxidized Cu_A. However, the most oxidized spectrum at 394 mV does not show an absorption peak at 830 nm (Fig. 1 *B*). The appearance of a broad peak in the difference spectrum is enhanced by a concavity in this spectral region shown in the most reduced spectrum at 124 mV (Fig. 1 *B*). In a separate experiment covering a wider spectral region to include the characteristic 605 nm α peak as a reference, a broad absorbance feature near 830 nm

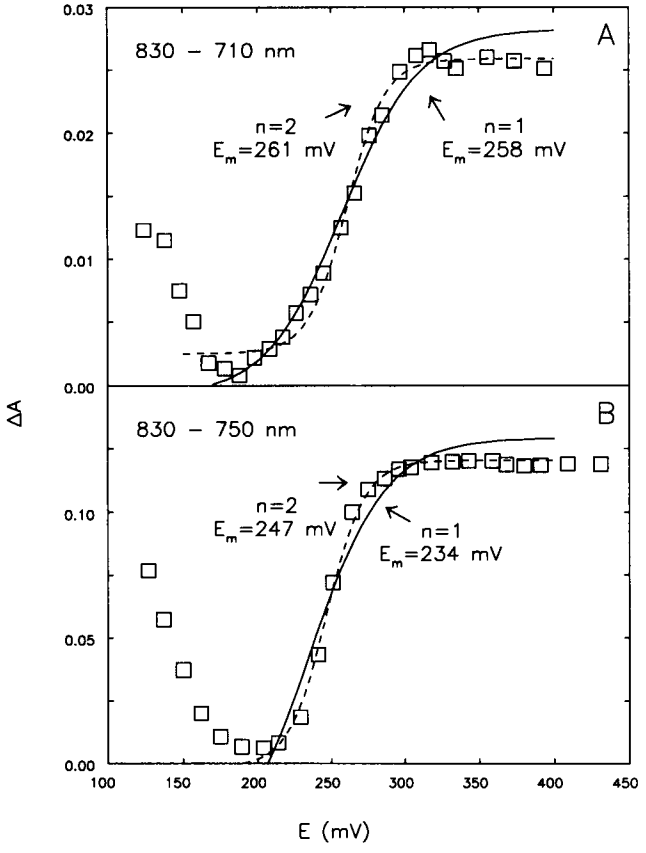

FIGURE 3 Potentiometric titrations of the 830 nm absorption feature. (*A*) The ΔA (830–710 nm) for the experiment shown in Fig. 1 is plotted against the solution potential. (*B*) The ΔA (830–750 nm) for the experiment shown in Fig. 2 is plotted against solution potential. The solid lines show fits to single, $n = 1$, Nernstian components, and the dashed lines to single Nernstian, $n = 2$, components.

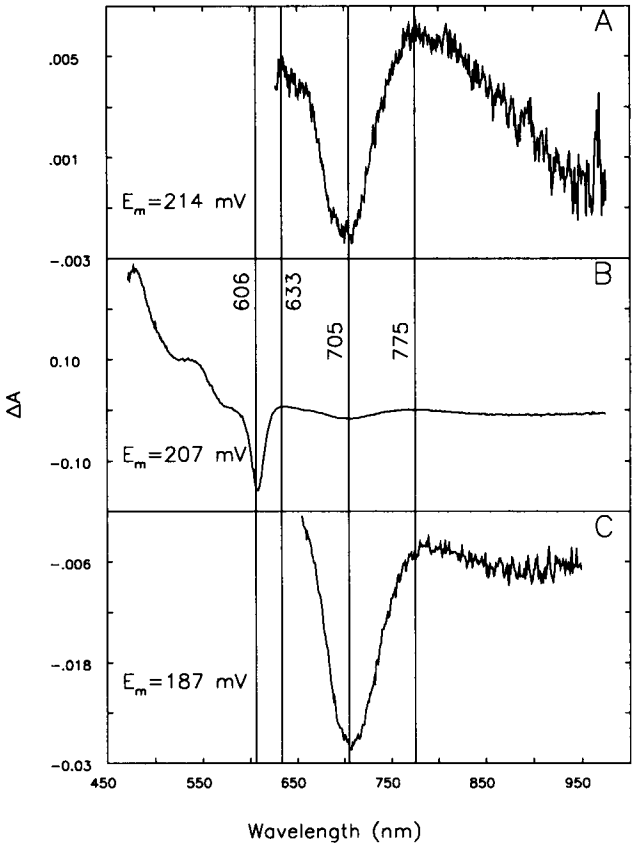

FIGURE 4 SVD-constructed difference spectra for the voltage transition near 200 mV. (*A*) Transition at $E_m = 214$ mV, from the data of the experiment shown in Fig. 1. (*B*) Transition at $E_m = 207$ mV, from the full data of the experiment shown in Fig. 2. Compare with Fig. 9 *A*. (*C*) Transition at $E_m = 187$ mV, from the restricted data (650–875 nm) of the experiment shown in Fig. 2. Compare with Fig. 9 *B*.

TABLE 1 Summary of the data for oxidized (−) reduced spectra

E_m (mV)	Spectral features (nm)					Figure number	Heme type
	tr.	pk.	tr.	tr.	pk.		
~200	606	633	705		775	4	a_3
~260	606	633		750		5	a
~285	606	633			775	6	a_3
~330	604	633		760		7	a
~390	604	633	705			8	?

Note: the shaded blocks in columns 5, 6, and 8 are meant to indicate a possible correlation between cytochrome a_3 and the peak at ~775 nm and between cytochrome a and the trough at ~750 nm. tr. and pk. refer to trough and peak, respectively.

in the oxidized minus reduced difference spectrum is again seen (Fig. 2 *A*). The absolute spectra show the relative magnitudes of the absorbance features near 605 and 830 nm and again demonstrate that there is no prominent absorbance feature at 830 nm in the most oxidized spectrum at 431 mV (Fig. 2 *B*). A concavity in the reduced spectrum in this spectral region is seen. Although the oxidized spectra shown in Figs. 1 and 2 are generally quite similar, it should be noticed that the reduced spectrum in Fig. 2 shows a more prominent broad absorbance near 750 nm than does the corresponding spectrum in Fig. 1. The major difference between the conditions of the two experiments is that the concentrations of cytochrome oxidase and mediators were doubled in the experiment depicted in Fig. 2 and hydroxymethylferrocene was substituted for $K_3Fe(CN)_6$. The broad feature near 750 nm was also seen in the experiment depicted in Fig. 1 in the SVD-reconstructed difference spectra (see Figs. 5 and 7) and in an actual difference spectrum in the appropriate voltage region using the raw data from the $K_3Fe(CN)_6$-mediated experiment (not shown). We have no explanation for the enhancement of this spectral feature under the conditions of the second experiment.

From the difference spectrum in Fig. 1, the two wavelength positions 710 and 830 nm were chosen as the basis for a ΔA data analysis to follow the redox behavior of the suggested Cu_A component. A plot of the magnitude of the ΔA (830–710 nm) vs. E for the experiment shown in Fig. 1 shows a decrease in the voltage range from 125 to 175 mV and then a rise in the higher voltage region, which has the appearance of a Nernstian titration (Fig. 3 *A*). The data in the voltage range 178 to 356 mV were fit by a single Nernst term with

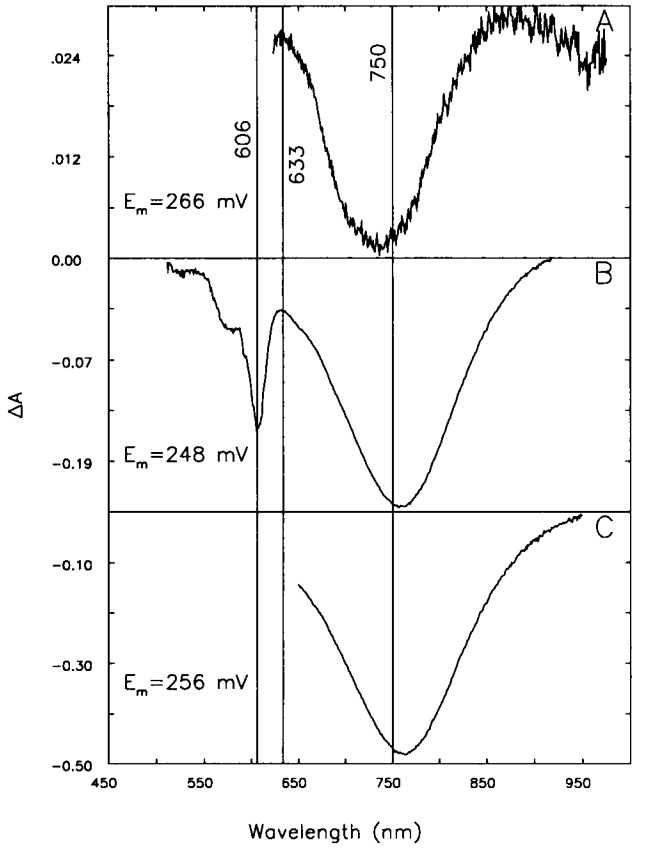

FIGURE 5 SVD-constructed difference spectra for the voltage transition near 260 mV. (*A*) Transition at E_m = 266 mV, from the data of the experiment shown in Fig. 1. (*B*) Transition at E_m = 248 mV, from the full data of the experiment shown in Fig. 2. Compare with Fig. 10 *A*. (*C*) Transition at E_m = 256 mV, from the restricted data (650–875 nm) of the experiment shown in Fig. 2. Compare with Fig. 10 *B*.

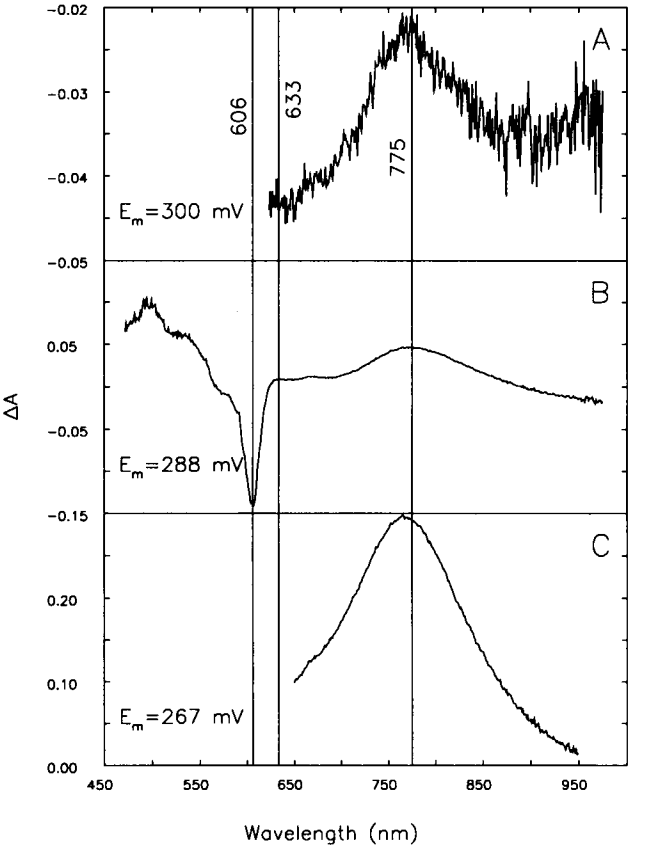

FIGURE 6 SVD-constructed difference spectra for the voltage transition near 285 mV. (*A*) Transition at E_m = 300 mV, from the data of the experiment shown in Fig. 1. (*B*) Transition at E_m = 288 mV, from the full data of the experiment shown in Fig. 2. Compare with Fig. 11 *A*. (*C*) Transition at E_m = 267 mV, from the restricted data (650–875 nm) of the experiment shown in Fig. 2. Compare with Fig. 11 *B*.

an E_m = 258 mV when n = 1 (*solid line*), and with an E_m = 261 mV when n = 2 (*dashed line*). From Fig. 2 *A*, it appears that 750 nm is a suitable reference wavelength for a ΔA analysis of the redox behavior at 830 nm in this experiment; the results of a plot of the ΔA (830–750 nm) are shown in Fig. 3 *B*. There is a drop in magnitude of ΔA in the voltage range 125 to ~180 mV and then a "Nernst-like" rise from 200–350 mV. The data in the range 204–343 mV were fit by a single Nernst with an E_m = 234 mV when n = 1 (*solid line*), and E_m = 247 mV when n = 2 (*dashed line*, Fig. 3 *B*). The apparent Nernstian behavior seen in the limited voltage ranges shown in Fig. 3 is indicative of the titration of a single species with a characteristic absorbance at ~830 nm. However, the oxidized absorption spectra in Figs. 1 and 2 do not show an isolated peak at 830 nm. The possibility is raised that rather than a single species (i.e., Cu_A), there is a mixture of several different spectral species reacting to changes in voltage and that sampling at 830 nm may reflect only a weighted average of these changes.

To explore this possibility, all of the spectral and voltage information available were analyzed by singular value decomposition (SVD). Five Nernstian transitions

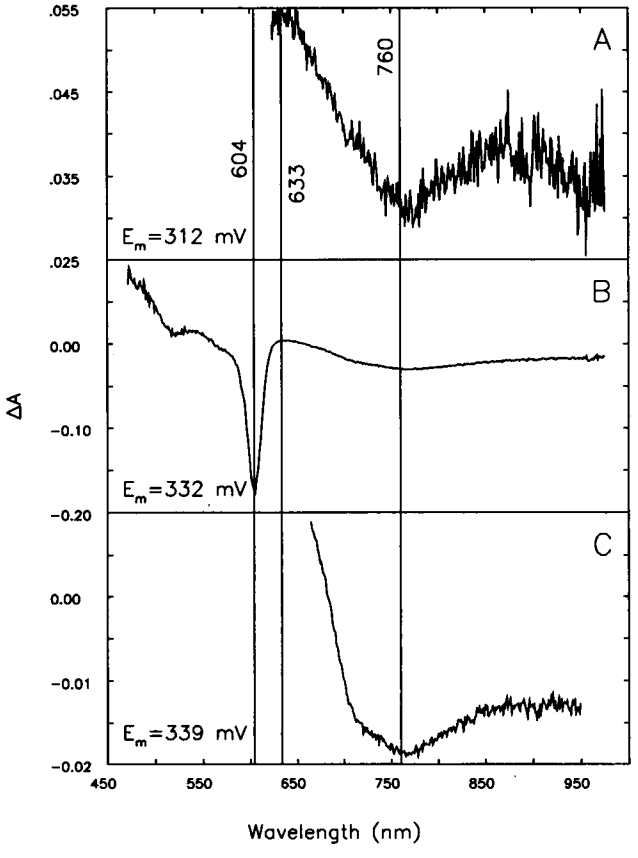

FIGURE 7 SVD-constructed difference spectra for the voltage transition near 330 mV. (*A*) Transition at E_m = 312 mV, from the data of the experiment shown in Fig. 1. (*B*) Transition at E_m = 322 mV, from the full data of the experiment shown in Fig. 2. Compare with Fig. 12 *A*. (*C*) Transition at E_m = 339 mV, from the restricted data (650–875 nm) of the experiment shown in Fig. 2. Compare with Fig. 12 *B*.

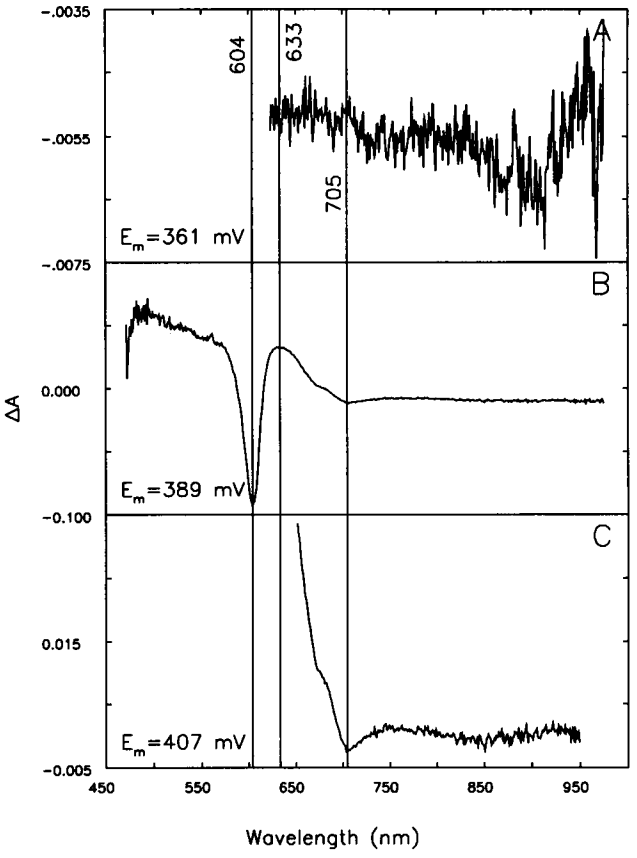

FIGURE 8 SVD-constructed difference spectra for the voltage transition near 390 mV. (*A*) Transition at E_m = 361 mV, from the data of the experiment shown in Fig. 1. (*B*) Transition at E_m = 389 mV, from the full data of the experiment shown in Fig. 2. Compare with Fig. 13 A. (*C*) Transition at E_m = 407 mV, from the restricted data (650–875 nm) of the experiment shown in Fig. 2. Compare with Fig. 13 *B*.

were distinguished in the voltage region of ~160–430 mV, with E_m values of ~200, ~260, ~285, ~330, and ~390 mV (Table 1). The SVD-deduced difference spectra associated with each of these transitions are shown in Figs. 4–8. The top panels in these figures were obtained from the complete experiment from which Fig. 1 was obtained. The middle panels were obtained from the complete experiment represented in Fig. 2. The bottom panels were obtained from a restricted spectral portion of the data used for the middle panels, to give greater weight to the changes affecting the weaker absorbance features in the near infrared region. To confirm that the SVD-deduced difference spectra did indeed represent the true spectral changes, actual difference spectra were derived from the raw data in the voltage ranges indicated by the fitted E_m values obtained in the SVD procedures (Figs. 9–13). It must be stressed that the actual difference spectra include overlaps of all the spectral changes occurring in the voltage gap examined, whereas SVD deduces changes for the individually titrating species. Therefore, it is to be expected that the major spectral changes will be similar in the SVD and actual difference spectra, but that the two sets may not be identical. The top and bottom

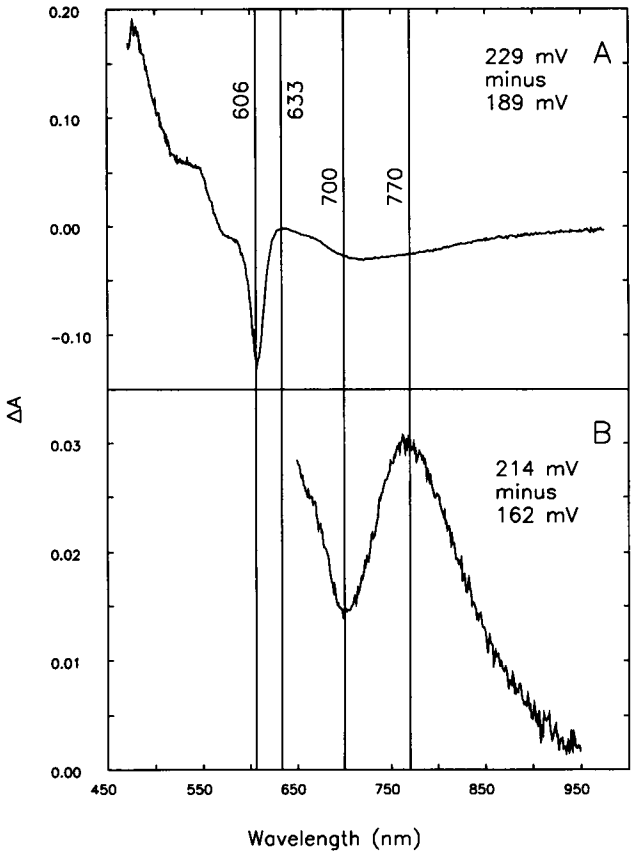

FIGURE 9 Actual difference spectra obtained from the data shown in Fig. 2 in the voltage regions corresponding to the SVD-deduced E_ms near 200 mV. (*A*) 229 mV minus 189 mV spectrum (compare with Fig. 4 *B*). (*B*) 214 mV minus 162 mV spectrum (compare with Fig. 4 *C*).

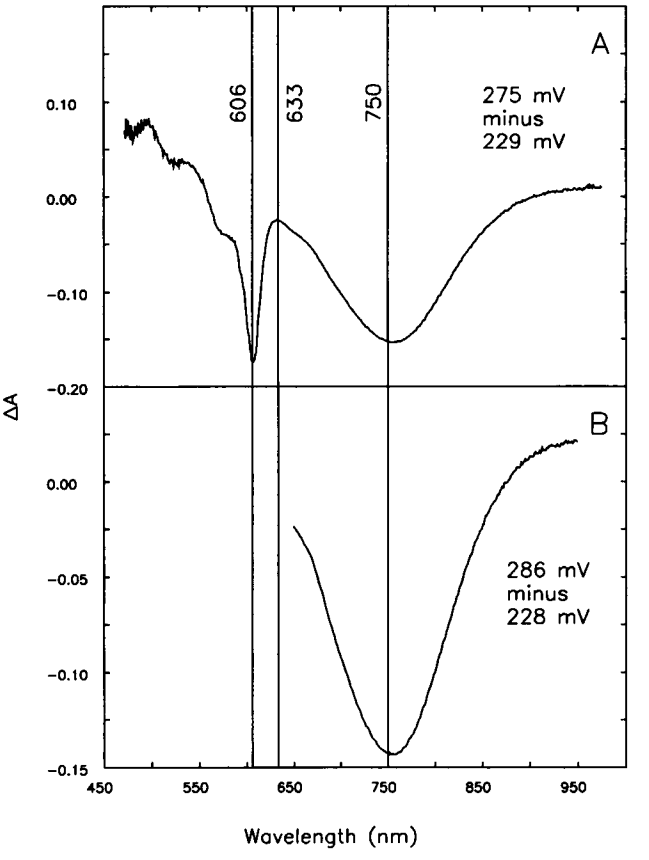

FIGURE 10 Actual difference spectra obtained from the data shown in Fig. 2 in the voltage regions corresponding to the SVD-deduced E_ms near 260 mV. (*A*) 275 mV minus 229 mV spectrum (compare with Fig. 5 *B*). (*B*) 286 mV minus 228 mV spectrum (compare with Fig. 5 *C*).

panels in Figs. 9–13 correspond to the middle and bottom panels in Figs. 4–8. It is seen that there is a good correspondence between the SVD-derived and the actual difference spectra in all cases. The most important point to note is that *there is a mixture of species being titrated, none of which shows a unique peak at 830 nm.*

A summary of all of the peaks and troughs seen in the SVD-derived spectra is presented in Table 1. Previous work has shown that the titrations occurring at ~200, ~260, and ~330 mV, as monitored by optical absorbance, are caused predominantly by cytochromes a_3, a, and a, respectively (Hendler and Westerhoff, 1994; Harmon et al., 1994a). In comparing the difference spectra for cytochrome a_3 at E_m near 200 mV (Fig. 4) and for cytochrome a at E_m near 260 mV (Fig. 5), and for cytochrome a at E_m near 330 mV, it is seen that a trough at ~705 nm and a peak at ~775 nm are characteristic of cytochrome a_3, whereas a trough at ~750 nm is characteristic of cytochrome a. Using these features as diagnostic, the titration at ~285 mV (Fig. 6) is seen to contain a contribution from cytochrome a_3 (i.e., the peak at ~775 nm). The presence of E_ms for both cytochromes a and a_3 close together near 250 mV, with that for a being about 30 mV lower than that for a_3, is entirely consistent with the recent findings obtained by potentiometry based on resonance Raman spectra (Harmon et al., 1994a). These studies found the E_ms to be 220 and 260 mV, respectively, for cytochromes a and a_3. However, when CN was used to isolate the titration of cytochrome a, an E_m of 260 mV was seen. Earlier (Hendler et al., 1986), it was shown that the addition of CO moved the E_m for cytochrome a from 260 to 243 mV. The existence of the two E_ms for cytochromes a and a_3 about 30 mV apart and near 250 mV is certain, although the exact values have not been established. The titration at ~390 mV (Fig. 8) shows a weak trough at ~705 nm, but the characteristic features at 750 and 775 nm are absent. This transition has been seen previously and attributed to cytochrome a because of its lack of sensitivity to CO (Pardhasaradhi et al., 1991; Hendler and Westerhoff, 1992). The apparent E_m for Cu_A, ~240 mV (Fig. 3) is closest to the species with E_m = ~260 mV obtained from the SVD analyses (Fig. 5). The difference spectra obtained for this transition, identified with cytochrome a, do not show a peak at 830 nm. The difference spectra in this voltage region (Fig. 10) also fail to reveal a peak at 830 nm. The closest the data

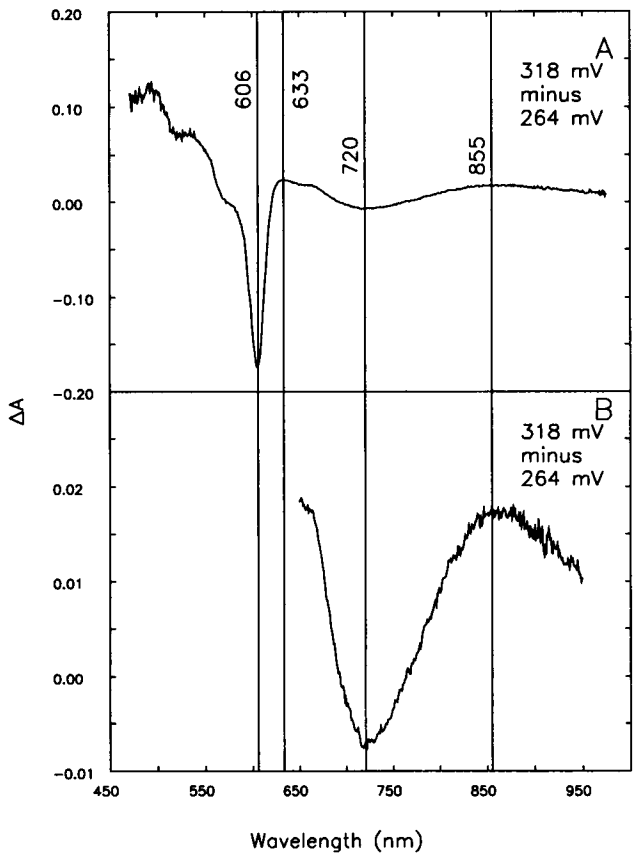

FIGURE 11 Actual difference spectra obtained from the data shown in Fig. 2 in the voltage regions corresponding to the SVD-deduced E_ms near 285 mV. (*A*) 318 mV minus 264 mV spectrum (compare with Fig. 6 *B*). (*B*) 318 mV minus 264 mV spectrum (compare with Fig. 6 *C*).

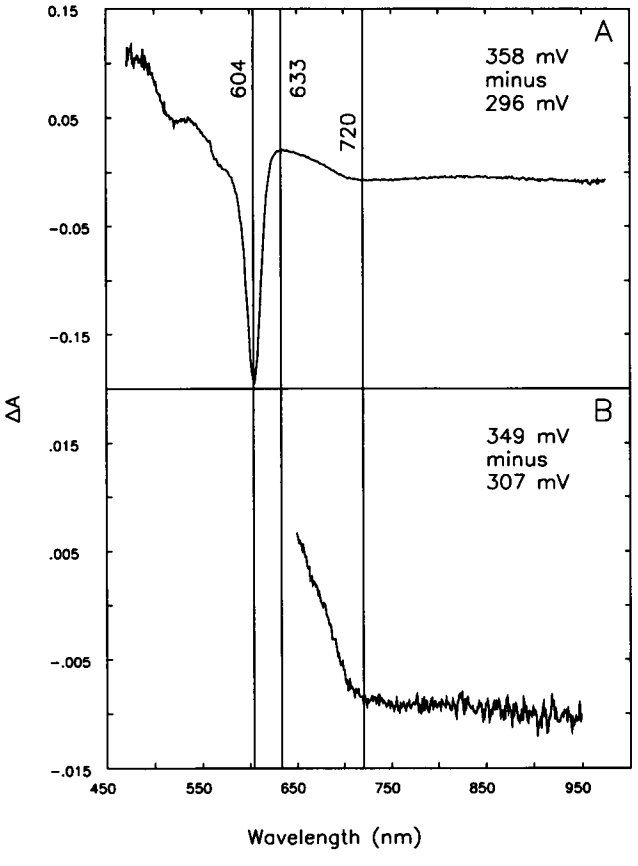

FIGURE 12 Actual difference spectra obtained from the data shown in Fig. 2 in the voltage regions corresponding to the SVD-deduced E_ms near 330 mV. (*A*) 358 mV minus 296 mV spectrum (compare with Fig. 7 *B*). (*B*) 349 mV minus 307 mV spectrum (compare with Fig. 7 *C*).

come to displaying a transition with a peak near 830 nm is in the difference spectrum from the raw data, centered at 290 mV(Fig. 11). This figure includes spectral contributions from more than a single species, and the central voltage position is not the same as the fitted values for "Cu_A" shown in Fig. 3.

DISCUSSION

Although, as described in the Introduction, the optical absorbance at 830 nm is widely used as a quantitative measure of the presence of oxidized Cu_A in cytochrome oxidase preparations, a proof that this is justified has not been presented. The strongest basis for the idea is the correlation of the redox behavior of the enzyme between the $g = 2$ signal in EPR and the optical absorbance at 830 nm. There is no question that copper is responsible for the EPR signal. That the optical absorbance is uniquely, or even preponderately, caused by Cu_A has not been demonstrated.

We have reproduced the observation that there is a Nernst-like titration of the 830 nm absorbance, if voltages below 200 mV are ignored (Fig. 3), and that its E_m is close to 240 mV, as reported by others (Tsudzuki and Wilson, 1971). Although others have reported that cytochromes *a* and a_3 do contribute to the absorbance in the 830 nm region (see Introduction), it has been generally believed that these contributions are quantitatively small. In the studies reported here, five redox species were identified. All of these displayed characteristic absorbances for cytochromes *a* and a_3. Based on previous studies, which identified a given species as belonging to either cytochrome *a* or a_3, a positive feature at ~775 mV in the oxidized minus reduced spectrum was associated with cytochrome a_3 and a trough at 750 nm with cytochrome *a*. Both Tsudzuki and Wilson (1971) and we in this work found that the E_m for Cu_A, using a 2-point ΔA centered at 830 nm and referenced to near 720 nm, is very close to that found for cytochrome *a*. Figs. 5 and 10 suggest a reasonable explanation for this in that the broad trough for cytochrome *a* centered at 750 nm contributes significantly to this ΔA.

It is obvious that the absorbance near 830 nm is not reserved for a single species. Most of the absorbance in this spectral region is associated with cytochromes *a* and a_3. In the absence of other independent studies that directly support the notion that the 830 nm absorbance is

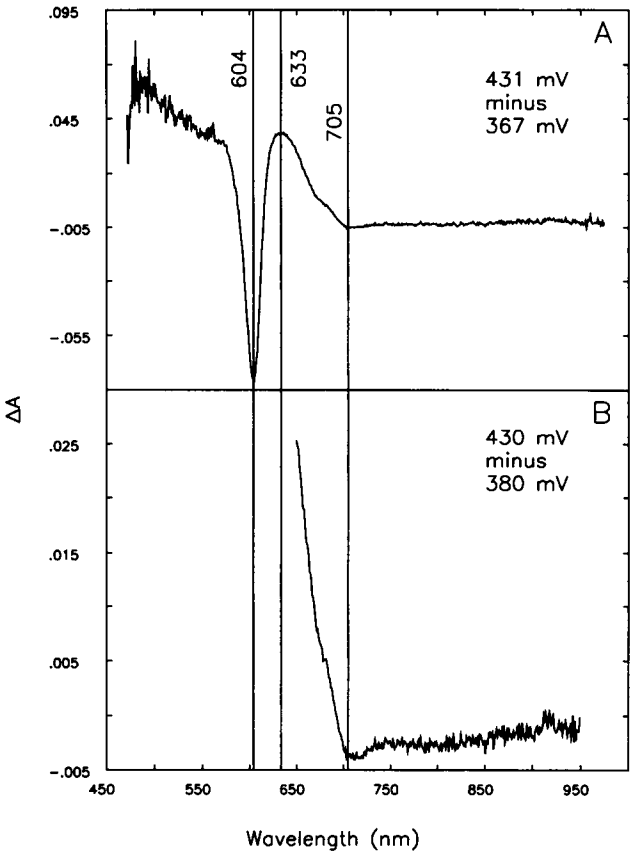

FIGURE 13 Actual difference spectra obtained from the data shown in Fig. 2 in the voltage regions corresponding to the SVD-deduced E_ms near 390 mV. (*A*) 431 mV minus 367 mV spectrum (compare with Fig. 8 *B*). (*B*) 430 mV minus 380 mV spectrum (compare with Fig. 8 *C*).

a dependable measure of Cu_A behavior, we recommend that conclusions based on this assumption be viewed with considerable caution.

REFERENCES

Beinert, H., R. W. Shaw, E. Hansen, and C. R. Hartzell. 1980. Studies on the origin of the near-infrared (800–900 nm) absorption of cytochrome *c* oxidase. *Biochim. Biophys. Acta.* 591:458–470.

Boelens, R., and R. Wever. 1980. Redox reactions in mixed-valence cytochrome *c* oxidase. *FEBS Lett.* 116:223–226.

Caughey, W. S., and S. McCoy. 1966. The Biochemistry of Copper. J. Peisach, P. Aisen, and W. E. Blumberg, editors. Academic Press, New York. 271–273.

Caughey, W. S., W. J. Wallace, J. A. Volpe, and S. Yoshikawa. 1976. The Enzymes, Vol. XIII, 3rd ed. P. D. Boyer, editor. Academic Press, New York. 299–344.

Einarsdottir, O., K. E. Georgiadis, and T. D. Dawes. 1992. Evidence for a band III analogue in the near-infrared absorption spectra of cytochrome *c* oxidase. *Biochem. Biophys. Res. Commun.* 184:1035–1041.

Eglinton, D. G., M. K. Johnson, A. J. Thomson, P. E. Gooding, and C. G. Greenwood. 1980. Near-infrared magnetic and natural circular dichroism of cytochrome *c* oxidase. *Biochem. J.* 191:319–331.

Greenwood, C., B. C. Hill, D. Barber, D. G. Eglinton, D. G., and A. J. Thomson. 1983. The optical properties of Cu_A in bovine cytochrome *c* oxidase determined by low-temperature magnetic-circular-dichroism spectroscopy. *Biochem. J.* 215:303–316.

Hallen, S., and P. Brzezinski. 1994. Light-induced structural changes in cytochrome *c* oxidase: implication for the mechanism of electron and proton gating. *Biochim. Biophys. Acta.* 1184:207–218.

Harmon, P. A., R. W. Hendler, and I. W. Levin. 1994a. Resonance Raman and optical spectroscopic monitoring of heme A redox states in cytochrome *c* oxidase during potentiometric titrations. *Biochem.* 33:699–707.

Harmon, P. A., R. W. Hendler, I. W. Levin, and W. Friauf. 1994b. Combination of potentiometry and resonance Raman spectroscopy for the analysis of a redox protein. *Anal. Biochem.* In press.

Hendler, R. W., and R. I. Shrager, 1994. Deconvolutions based on singular value decomposition and the pseudoinverse: a guide for beginners. *J. Biochem. Biophys. Methods.* 28:1–33.

Hendler, R. W., K. V. Subba Reddy, R. I. Shrager, and W. S. Caughey. 1986. Analysis of the spectra and redox properties of pure cytochromes aa_3. *Biophys. J.* 49:717–729.

Hendler, R. W., and H. V. Westerhoff. 1992. Redox interactions in cytochrome *c* oxidase: from the "neoclassical" toward "modern" models. *Biophys. J.* 63:1586–1604.

Hill, B. C. 1981. The reaction of the electrostatic cytochrome *c*-cytochrome oxidase complex with oxygen. *J. Biol. Chem.* 266:2219–2226.

Hill, B. C. 1994. Modeling of the sequence of electron transfer reactions in the single turnover of reduced, mammalian cytochrome *c* oxidase with oxygen. *J. Biol. Chem.* 269:2419–2425.

Morgan, J. E., P. M. Li, D-J. Jang, M. A. El-Sayed, and S. I. Chan. 1989. Electron transfer between cytochrome *a* and copper A in cytochrome *c* oxidase: a perturbed equilibrium study. *Biochemistry.* 28:6975–6983.

Rich, P. R., A. J. Moody, and W. J. Ingledew. 1992. Detection of a near infra-red absorption band of ferrohaem a_3 in cytochrome *c* oxidase. *FEBS Lett.* 305:171–173.

Thornstrom, P. E., P. Brzezinski, P. O. Fredriksson, and B. G. Malmström. 1988. Cytochrome *c* oxidase as an electron-transport-driven proton pump: pH dependence of the reduction levels of the redox centers during turnover. *Biochemistry.* 27:5441–5447.

Tiesjema, R. H., A. O. Muijsers, and B. F. Van Gelder. 1973. Biochemical and biophysical studies on cytochrome *c* oxidase. X. Spectral and potentiometric properties of the hemes and coppers. *Biochim. Biophys. Acta.* 305:19–28.

Tsudzuki, T., and D. F. Wilson. 1971. The oxidation-reduction potentials of the hemes and copper of cytochrome oxidase from beef heart. *Arch. Biochem. Biophys.* 145:149–154.

Wharton, D. C. 1964. Valence state of copper after interaction of the cytochrome oxidase-carbon monoxide complex with ferricyanide. *Biochim. Biophys. Acta.* 92:607–609.

Wharton, D. C., and A. Tzagaloff. 1964. Studies on the electron transfer system. LVII. The near infrared absorption band of cytochrome oxidase. *J. Biol. Chem.* 239:2036–2041.

Wikström, M., K. Krab, and M. Saraste. 1981. Cytochrome Oxidase: A synthesis. Academic Press, London.

Yoshikawa, S., M. G. Choc, M. C. O-Toole, and W. S. Caughey. 1977. An Infrared study of CO binding to the heart cytochrome *c* oxidase and hemoglobin A. *J. Biol. Chem.* 252:5498–5508.